British Journal of Pharmacology (2005) 145, 34–42
www.nature.com/bjp

Mechanisms of inverse agonist action at D_2 dopamine receptors

[1]David J. Roberts & *,[1]Philip G. Strange

[1]School of Animal and Microbial Sciences, University of Reading, Whiteknights, Reading RG6 6AJ

1 Mechanisms of inverse agonist action at the $D_{2(short)}$ dopamine receptor have been examined.

2 Discrimination of G-protein-coupled and -uncoupled forms of the receptor by inverse agonists was examined in competition ligand-binding studies *versus* the agonist [^{3}H]NPA at a concentration labelling both G-protein-coupled and -uncoupled receptors.

3 Competition of inverse agonists *versus* [^{3}H]NPA gave data that were fitted best by a two-binding site model in the absence of GTP but by a one-binding site model in the presence of GTP. K_i values were derived from the competition data for binding of the inverse agonists to G-protein-uncoupled and -coupled receptors. $K_{coupled}$ and $K_{uncoupled}$ were statistically different for the set of compounds tested (ANOVA) but the individual values were different in a *post hoc* test only for (+)-butaclamol.

4 These observations were supported by simulations of these competition experiments according to the extended ternary complex model.

5 Inverse agonist efficacy of the ligands was assessed from their ability to reduce agonist-independent [^{35}S]GTPγS binding to varying degrees in concentration–response curves. Inverse agonism by (+)-butaclamol and spiperone occurred at higher potency when GDP was added to assays, whereas the potency of (−)-sulpiride was unaffected.

6 These data show that some inverse agonists ((+)-butaclamol, spiperone) achieve inverse agonism by stabilising the uncoupled form of the receptor at the expense of the coupled form. For other compounds tested, we were unable to define the mechanism.
British Journal of Pharmacology (2005) **145,** 34–42. doi:10.1038/sj.bjp.0706073
Published online 28 February 2005

Keywords: Inverse agonism; mechanism; ligand binding; [^{35}S]GTPγS binding; receptor/G-protein interaction

Abbreviations: NPA, N-propylnorapomorphine; $\%R_H$, % of higher affinity sites; [^{35}S]GTPγS, guanosine-5′-*O*-(3-[^{35}S]thiotriphosphate)

Introduction

It is now a common observation that ligands previously classified as antagonists have the ability to inhibit agonist-independent activation of receptors. They, therefore, act as inverse agonists in systems that are sufficiently sensitive to allow detection. This was first shown in work on opiate and α_2-adrenergic receptors (Costa & Herz, 1989; Costa *et al*., 1992; Tian *et al*., 1994), where it was suggested that some antagonists could reduce agonist-independent G-protein-coupled receptor (GPCR) activation. These observations have therapeutic considerations in the case of administration of drugs previously thought to act as antagonists, but which have now been classified as inverse agonists and which may have additional effects. For example, prolonged use of the histamine H_2 receptor inverse agonist, cimetidine, produces tolerance and an increased sensitivity to histamine upon withdrawal (Alewijnse *et al*., 1998) which may be due to upregulation of the receptors. Also, in the treatment of schizophrenia, the drugs used (antipsychotics) were assumed to be antagonists at the D_2 dopamine receptor. It has since been shown using inhibition of guanosine-5′-*O*-(3-[^{35}S]thiotriphosphate) ([^{35}S]GTPγS) binding (Wiens *et al*., 1998) and potentiation of adenylyl cyclase activity (Hall & Strange, 1997; Kozell & Neve, 1997; Wilson *et al*., 2001; Akam & Strange, 2004) that all the antipsychotics tested so far are inverse agonists. The increased numbers of histamine H_2 receptors observed after prolonged cimetidine treatment and D_2 dopamine receptors seen upon chronic antipsychotic treatment may be a reflection of this inverse agonist property of the drugs.

Inverse agonist activity at GPCRs has been described in the context of the extended ternary complex model (Figure 1) (Lefkowitz *et al*., 1993; Samama *et al*., 1993). In this model, the receptor exists in an inactive (R) state, which can isomerise to the partially active (R*) state that couples efficiently to G-proteins (R*G). Inverse agonists have, therefore, been proposed to stabilise the 'R' state, reducing agonist-independent G-protein activation. Alternatively, inverse agonists may stabilise the G-protein-uncoupled states of the receptor (R/R* states) in preference to the G-protein-coupled state (R*G) (Costa *et al*., 1992; McLoughlin & Strange, 2000). In either case, inverse agonists would be expected to exhibit different affinities for different states of the receptor in ligand-binding assays, provided formation of the activated states is favourable. Also, the functional effects of inverse agonists should be sensitive to the effects of agents that redistribute different states of the receptor such as GTP or GDP. Where inverse agonists show no discrimination for the different states of the receptor in ligand-binding and functional assays, other

*Author for correspondence; E-mail: p.g.strange@reading.ac.uk
Published online 28 February 2005

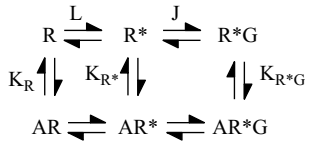

Figure 1 Extended ternary complex model. The model is shown for a receptor existing in ground (R), partially activated (R*) and fully active, G-protein-coupled states (R*G). The equilibrium constants governing the R/R* and R*/R*G transitions are L and J, respectively. The equilibrium constants for agonist binding to R, R* and R*G are K_R, K_{R^*} and K_{R^*G}, respectively.

mechanisms may operate. The inverse agonist methiothepin, acting at the 5-HT_{1A} receptor, displays no affinity preference in competition against a radiolabelled agonist or inverse agonist, while another inverse agonist, spiperone, did show such discrimination (McLoughlin & Strange, 2000). Likewise, no affinity preference for a selection of inverse agonists acting at the D_2 receptor could be determined using a similar method with agonist and inverse agonist radioligands (Roberts *et al*., 2004). It has been postulated that the lack of discrimination results from the inverse agonist binding to a receptor conformation that does not induce a redistribution of the R/R*/R*G states but nonetheless inactivates the receptor (Gether & Kobilka, 1998; Strange, 2002) or sequesters G-proteins in an inactive state (Bouaboula *et al*., 1997; 1999).

It is important to understand the mechanisms of inverse agonist action at the D_2 dopamine receptor as many of the drugs used to treat schizophrenia are inverse agonists. The drugs are used chronically and their therapeutic mechanisms may depend on this inverse agonism (Strange, 2001). The aim of this work, therefore, was to probe the mechanisms of action of a range of inverse agonists at D_2 receptors by labelling G-protein-coupled and -uncoupled states of the receptor with the agonist [^{3}H]N-propylnorapomorphine ([^{3}H]NPA) (Sibley *et al*., 1982). This enables inverse agonist affinities for the two states to be determined in a single ligand-binding assay. The relative efficacy of the inverse agonists was also determined by measuring the reduction of basal [^{35}S]GTPγS binding. Data were then compared with the predictions arising from the two mechanisms outlined above. The results show that some inverse agonists at the D_2 receptor may exert their effects through preferential binding to the ground state of the receptor (R), whereas for other inverse agonists we are unable to distinguish the two mechanisms outlined earlier.

Methods

Materials

[^{35}S]GTPγS ($\sim$37 TBq mmol^{-1}) was purchased from Amersham Biosciences (Buckinghamshire, U.K.). [^{3}H]NPA ($\sim$1 TBq mmol^{-1}) and Optiphase HiSafe-3 scintillation fluid was purchased from Perkin-Elmer Life Sciences (Cambridge, U.K.). Dopamine was purchased from TOCRIS (Bristol, U.K.). (+)-Butaclamol, clozapine, GTP, haloperidol, raclopride, (−)-sulpiride and spiperone were purchased from Sigma (Dorset, U.K.). Risperidone, quetiapine and ziprasidone were gifts from Janssen (Beerse, Belgium), AstraZeneca (Macclesfield, U.K.) and Psychiatry CEDD, Glaxo SmithKline (Harlow, U.K.), respectively.

Cell culture

CHO cells stably expressing human D_{2short} dopamine receptors (Wilson *et al*., 2001) were grown in Dulbecco's modified Eagle's medium containing 5% foetal bovine serum and 400 μg ml^{-1} active geneticin at 37°C in an humidified atmosphere of 5% CO_2.

Membrane preparation

Membranes were prepared from CHO cells expressing D_{2short} dopamine receptors as described previously (Castro & Strange, 1993). Briefly, confluent 175 cm^2 flasks of cells were washed once with 5 ml HEPES buffer (20 mM HEPES, 1 mM EGTA, 1 mM EDTA, 10 mM $MgCl_2$; pH 7.4). Cells were then removed from the surface of the flasks using 5 ml HEPES buffer and glass balls (2 mm diameter) and were then homogenised using an Ultra-Turrax homogeniser (two 5 s treatments). The homogenate was centrifuged at 1700 × *g* (10 min, 4°C), after which the supernatant was centrifuged at 48,000 × *g* (60 min; 4°C). The resulting pellet was resuspended in HEPES buffer at a concentration of 3–5 mg protein ml^{-1} (determined by the method of Lowry *et al*., 1951) and stored in aliquots at −70°C until use.

Radioligand-binding assays

Cell membranes (25 μg membrane protein) were incubated with [^{3}H]NPA (30 pM–10 nM for saturation experiments, 1 nM for competition experiments) and competing drugs in HEPES buffer (containing 100 mM *N*-methyl D-glucamine and 0.1 mM dithiothreitol) in a final volume of 1 ml for 3 h at 25°C. In saturation experiments, nonspecific binding was determined in the presence of 3 μM (+)-butaclamol, whereas in competition experiments nonspecific binding was determined as the maximal inhibition of [^{3}H]NPA binding by the ligand, which was equivalent for all ligands tested. The assay was terminated by rapid filtration (through Whatman GF/C filters) using a Brandel cell harvester followed by four washes with 4 ml ice-cold phosphate-buffered saline (0.14 M NaCl, 3 mM KCl, 1.5 mM KH_2PO_4, 5 mM Na_2HPO_4; pH 7.4) to remove unbound radioactivity. Filters were soaked in 2 ml Optiphase HiSafe-3 for at least 5 h and bound radioactivity was determined by liquid scintillation counting.

[^{35}S]GTPγS-binding assays

Cell membranes (25 μg membrane protein) were incubated with ligands in triplicate in a volume of 0.9 ml of HEPES buffer containing *N*-methyl D-glucamine (100 mM) and no GDP (unless specified otherwise) for 20 min at 30°C. The reaction was initiated with the addition of 100 μl [^{35}S]GTPγS diluted to give a final concentration of 100 pM. The assay was incubated for a further 30 min before termination by rapid filtration as above. The relative efficacy of inverse agonists was determined by reference to that of (+)-butaclamol for which a full inverse agonist activity curve was included in each experiment.

Simulations of data using the extended ternary complex model

Simulations were performed in Excel using the extended ternary complex model (Figure 1) with two competing ligands. G-protein concentration (50 nM) was assumed to be half that of receptor concentration (100 nM) to allow for the ~50% G-protein-coupled state normally observed in competition-binding experiments with agonists (Gardner *et al*., 1997). A value of 100 was used for L, indicating that R* formation was unfavourable, while J was varied to examine the effect of changing R*G stability. Data were simulated in Excel as described in the legend to Figures 5 and 6 and Table 4, and were fitted using GraphPad Prism (GraphPad Inc., San Diego, CA, U.S.A.). The Excel spreadsheet with the extended ternary complex model was derived by Dr Claire Carter (née Scaramellini) as in Leff *et al*. (1997) and the equations were derived using a method similar to that used in Alder *et al*. (2003).

Data analysis

Radioligand-binding data were analysed using Prism. Saturation- and competition-binding experiments were assumed to fit best to a one-binding site model unless a two-binding site model provided a statistically better fit; statistical significance was determined using an *F*-test ($P<0.05$). Inhibition constants were calculated from IC_{50} values in competition experiments using the Cheng–Prusoff equation (Cheng & Prusoff, 1973) using the respective K_d values for [^{3}H]NPA for the coupled and uncoupled states as described in the Results section. Statistical comparisons between values within a data set were carried out using one-way ANOVA and comparisons between two data sets were carried out using an unpaired two-way ANOVA followed by a Bonferroni *post hoc* test with the significance determined as $P<0.05$. For the dissociation constants, pK values were used in these comparisons. The data on the effects of GDP on inverse agonist potency were also analysed using linear regression.

Results

Binding of inverse agonists determined in competition versus *the agonist [^{3}H]NPA*

[^{3}H]NPA binding to D_2 receptors expressed in CHO cell membranes occurred in a saturable manner and the data were fitted best by a two-binding site model. Dissociation constants were: pK_h 10.27±0.08 (0.05 nM) and pK_l 9.09±0.06 (0.82 nM) (mean±s.e.m., $n=4$) and the higher affinity sites represented 40±6% of the total population; B_{max} 0.96±0.06 pmol mg^{-1}. When saturation-binding assays with [^{3}H]NPA were performed in the presence of GTP (100 μM), the data were fitted best by a one-binding site model (pK_d 9.04±0.06 (mean± s.e.m., $n=4$)), pK_d and pK_l were not significantly different ($P>0.05$).

Competition-binding experiments were carried out using a panel of inverse agonists *versus* the binding of [^{3}H]NPA at a concentration of 1 nM. This concentration is sufficient to label both higher- and lower-affinity receptor sites. Competition curves were constructed with three concentrations of competitor per log unit in order to define the curves well. Competition curves stretched over four log units and were characterised by Hill coefficients less than one. Data for all of the inverse agonists tested were fitted best by a two-binding site model, indicative of competition with [^{3}H]NPA at both higher- and lower-affinity binding sites (Figure 2a). Competition curves, obtained in the absence of GTP, were analysed to provide IC_{50} values for the inverse agonists at the two sites and the percentage of receptors in the higher affinity state. These IC_{50} values differed by up to 20-fold. Upon addition of 100 μM GTP, competition data for inverse agonists were fitted best by a one-binding site model, consistent with competition of [^{3}H]NPA from binding sites uncoupled from G-protein (Figure 2b). IC_{50} values for inverse agonists in the presence of GTP were similar to the IC_{50} values of the higher-affinity sites observed in the absence of GTP ($P>0.05$). The IC_{50} values were then converted to inhibition constants (K_i).

In this analysis, it was assumed that the higher- and lower-affinity [^{3}H]NPA binding sites corresponded to G-protein-coupled and -uncoupled states, respectively. It was also assumed that, for the inverse agonists, the higher-affinity component in the competition curve corresponded to the G-protein-uncoupled state of the receptor. This assumption is based on the correspondence between the IC_{50} for the higher-affinity state in the competition curve in the absence of GTP and the single IC_{50} value observed in competition analyses for the presence of GTP. Values for $K_{coupled}$ and $K_{uncoupled}$ for inverse agonists were then determined assuming simple competition (using the corresponding K_d values for [^{3}H]NPA for the two states) and are given in Table 1. $K_{uncoupled}$ obtained

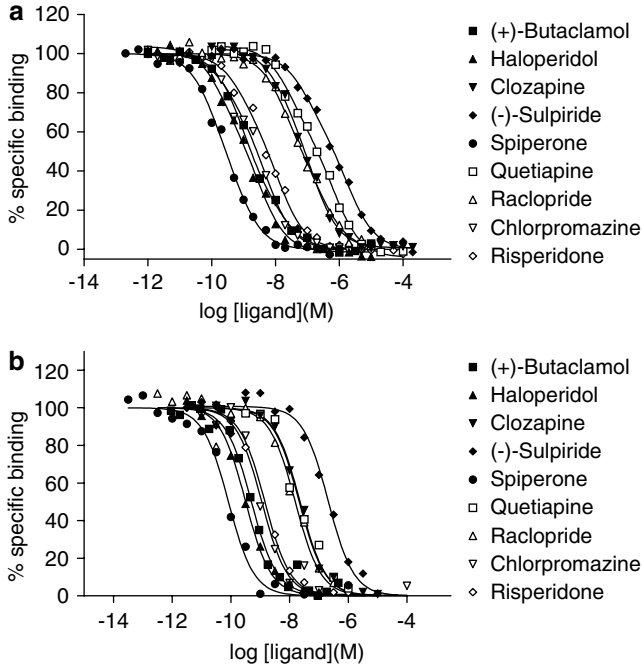

Figure 2 Binding of inverse agonists to dopamine D_2 receptors expressed in CHO cells. Inverse agonist binding was determined in competition *versus* (a) 1 nM [^{3}H]NPA or (b) 1 nM [^{3}H]NPA and 100 μM GTP, as described in Methods section. Data in (a) were best fitted by a two-binding site model, while those in (b) were best fitted by a one-binding site model. Curves shown are representative examples of data replicated as in Table 1.

Table 1 Dissociation constants of inverse agonists for binding to D_2 dopamine receptors

	$pK_{uncoupled}$ ($K_{uncoupled}$, nM)	$pK_{coupled}$ ($K_{coupled}$, nM)	$\%R_{high}$	pK_{iGTP} (K_{iGTP}, nM)	*Hill slope* (−, + *GTP*)	$n=-,+$ GTP
(+)-Butaclamol	9.41±0.08	8.86±0.09*	77±3	9.46±0.21**	−0.74±0.02	5,3
	(0.39)	(1.4)		(0.35)	−1.21±0.19	
Chlorpromazine	9.77±0.23	9.46±0.12	47±12	9.53±0.08	−0.73±0.03	4,4
	(0.16)	(0.35)		(0.29)	−0.90±0.12	
Clozapine	8.26±0.16	8.12±0.12	34±9***,†	8.09±0.07	−0.80±0.04	4,4
	(5.5)	(7.6)		(8.1)	−0.97±0.06	
Haloperidol	9.90±0.06	9.76±0.03	48±3	9.90±0.04	−0.75±0.02	4,4
	(0.13)	(0.17)		(0.13)	−0.81±0.05	
Quetiapine	8.17±0.11	7.72±0.08	38±4***,†	7.73±0.14	−0.68±0.03	4,4
	(6.8)	(19.0)		(18.6)	−0.90±0.07	
Raclopride	8.74±0.29	8.40±0.27	45±7***	8.72±0.31	−0.69±0.02	4,4
	(1.8)	(4.00)		(1.9)	−0.86±0.05	
Risperidone	9.35±0.12	9.13±0.05	42±8***	9.15±0.07	−0.74±0.01	4,3
	(0.45)	(0.74)		(0.71)	−0.83±0.03	
Spiperone	10.11±0.07	9.97±0.20	72±8	10.37±0.06	−0.86±0.01	4,4
	(0.08)	(0.11)		(0.04)	−1.21±0.10	
(−)-Sulpiride	7.30±0.11	6.96±0.07	42±4***,†	7.19±0.06	−0.68±0.02	5,4
	(50.1)	(109.6)		(64.5)	−0.80±0.03	

Competition-binding experiments were performed using membranes of CHO cells expressing D_2 receptors for the inverse agonists *versus* [^{3}H]NPA (1 nM) in the presence or absence of 100 μM GTP, as described in Methods section. In the absence of GTP, competition curves were fitted best by a two-binding site model from which values for $K_{\text{uncoupled}}$ and K_{coupled} and the percentage of higher-affinity states (% R_{high}) were derived as described in the text. In the presence of GTP, data were fitted best by a one-binding site model from which values of K_{iGTP} were derived. The Hill slopes for the competition curves are also shown. Values for parameters are expressed as mean±s.e.m. from *n* experiments.

*$P<0.05$ comparing pK_{coupled} and p$K_{\text{uncoupled}}$ values.

**$P<0.05$ comparing pK_{coupled} with pK_{iGTP} values.

***$P<0.05$ comparing the percentage in high affinity to that of (+)-butaclamol.

†$P<0.05$ comparing the percentage in high affinity to that of spiperone.

from the experiments in the absence of GTP was compared with the K_i values obtained in the presence of GTP (K_{iGTP}). The two sets of data were not significantly different ($P<0.05$). Statistical comparison of K_{iGTP} with K_{coupled} showed a significant difference between the data sets ($P<0.05$). Statistical comparison of K_{coupled} and $K_{\text{uncoupled}}$ values showed a significant difference between the data sets (ANOVA, $P<0.05$). For most ligands, $K_{\text{coupled}}/K_{\text{uncoupled}}\sim 2$. For clozapine and sulpiride, however, this ratio was lower ($K_{\text{coupled}}/K_{\text{uncoupled}}\sim 1.3$), whereas for (+)-butaclamol $K_{\text{coupled}}/K_{\text{uncoupled}}$ was $\sim$4 and this was significantly different in a *post hoc* test. Statistical comparison of K_{coupled} and $K_{\text{uncoupled}}$ values without the data for (+)-butaclamol also showed a significant difference between the data sets (ANOVA, $P<0.05$) but no compound was significantly different in a *post hoc* test. The percentage of receptors in the higher-affinity form, which represents G-protein-uncoupled receptor, was variable. For most inverse agonists, higher-affinity binding sites constituted 40–50% of the total [^{3}H]NPA binding. For spiperone and (+)-butaclamol, however, higher-affinity binding sites constituted more (70–80%) of the total [^{3}H]NPA binding ($P<0.05$).

Based on these analyses of the data, it seems that the percentage of higher-affinity sites depends on the ligand tested. This is not to be expected from the extended ternary complex model and so we investigated whether constraining the parameters in curve fitting would alter the analyses. Binding curves were, therefore, fitted with the percentage of higher-affinity sites ($\%R_H$) constrained to 43% (the mean $\%R_H$ in Table 1), to 47% (the estimated occupancy of uncoupled sites by [^{3}H]NPA at 1 nM) and to 60% (the percentage of uncoupled sites in [^{3}H]NPA saturation analyses). When these analyses were performed, data for clozapine, quetiapine, raclopride and sulpiride were fitted best with $\%R_H$ constrained to 43%, whereas data for haloperidol and risperidone were fitted best with $\%R_H$ constrained to 47% and data for chlorpromazine and spiperone were fitted best with $\%R_H$ constrained to 60%. None of these constraints provided a better fit for (+)-butaclamol. When the parameters derived from the best fits were analysed, the statistics were unaltered, with the exception of the comparison of K_{coupled} and IC_{50} in [^{35}S]GTPγS-binding assays ($P<0.05$) (see below).

Inhibition of [^{35}S]GTPγS binding by inverse agonists

The effects of inverse agonists to inhibit agonist-independent [^{35}S]GTPγS binding were determined in concentration/response experiments. Each of the compounds tested inhibited [^{35}S]GTPγS binding by 15–20% and the maximal effect (relative to the maximal (+)-butaclamol effect) and the potency (IC_{50}) were determined (Table 2; Figure 3). It was found that some of the inverse agonists tested (spiperone, haloperidol, clozapine and chlorpromazine) showed high relative efficacy (80–100% of the maximal response to (+)-butaclamol), while others (quetiapine, raclopride, sulpiride) showed a significantly lower relative efficacy (>60%, $P<0.05$). A statistical comparison between the IC_{50} and K_{coupled} data sets in Table 1 showed no significant difference between them ($P>0.05$). Conversely, there was a significant difference between the IC_{50} and $K_{\text{uncoupled}}$ data sets ($P<0.001$). When the ligand-binding parameters derived from additional data analyses (see above) were used, IC_{50} and K_{coupled} were found to be significantly different ($P<0.05$).

Table 2 Inhibition of [^{35}S]GTPγS binding by inverse agonists

	pIC_{50} (IC_{50}, nM)	% of (+)-butaclamol response	n
(+)-Butaclamol	9.28±0.16 (0.53)	100	11
Chlorpromazine	8.66±0.33 (2.2)	89±8	6
Clozapine	7.30±0.14 (50.1)	86±2	4
Haloperidol	9.54±0.10 (0.29)	83±6	5
Quetiapine	7.52±0.24 (30.2)	73±4*	4
Raclopride	8.51±0.14 (3.1)	61±19*	4
Risperidone	9.25±0.21 (0.56)	92±8	5
Spiperone	9.67±0.10 (0.21)	93±4	5
(−)-Sulpiride	6.87±0.07 (134.9)	65±4*	5
Ziprasidone	9.27±0.10 (0.54)	95±7	4

Inhibition of [^{35}S]GTPγS binding to membranes of CHO-D_2 cells by inverse agonists was determined as described in Methods section. Concentration/response experiments were performed and IC_{50} and maximal effects determined. Maximal responses were expressed as a percentage of the maximum response from (+)-butaclamol. Values are expressed as mean±s.e.m. from *n* experiments.
*$P<0.05$ compared to (+)-butaclamol.

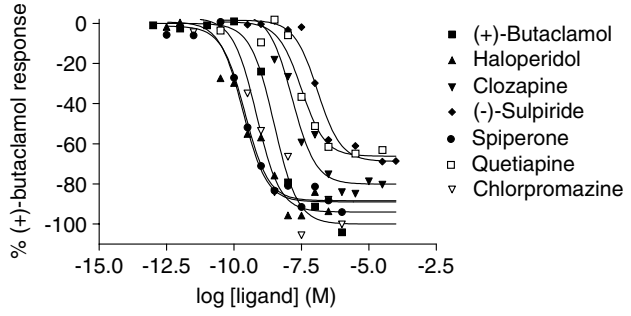

Figure 3 Inhibition of basal [^{35}S]GTPγS binding by inverse agonists *via* D_2 dopamine receptors expressed in CHO cells. [^{35}S]GTPγS binding was determined in the presence of different concentrations of drugs as described in Methods section. The data were fitted using a sigmoidal dose–response curve with a Hill coefficient of one and expressed as a percentage of the maximal (+)-butaclamol response. The data shown represent single experiments, replicated as in Table 2.

Effect of increasing GDP concentration on inverse agonist potency for inhibition of [^{35}S]GTPγS binding

Concentration/response curves for (+)-butaclamol, spiperone and (−)-sulpiride were determined in the presence of increasing GDP concentrations to examine effects on ligand potency (Figure 4; Table 3). When the IC_{50} values were analysed using linear regression, a significant relationship was found between IC_{50} and [GDP] for (+)-butaclamol and spiperone ($P<0.05$). When the IC_{50} values were compared, the IC_{50} for (+)-butaclamol as an inverse agonist did show a significant increase between 10 and 300 nM GDP (IC_{50}: 1.5–0.43 nM; ANOVA, $P<0.05$; Table 3). This increase was similar to the values of $K_{uncoupled}$ and $K_{coupled}$ determined using [^{3}H]NPA competition ($K_{coupled}$ 1.5 nM; $K_{uncoupled}$ 0.41 nM). However, no significant change in IC_{50} was found for either spiperone or (−)-sulpiride using this analysis ($P>0.05$). The values for maximal effects of inverse agonists decreased as the GDP concentration was increased (Table 3). We could not, therefore, extend the range of [GDP] used, as at concentrations above 300 nM the inverse agonist signal was too small for accurate analyses.

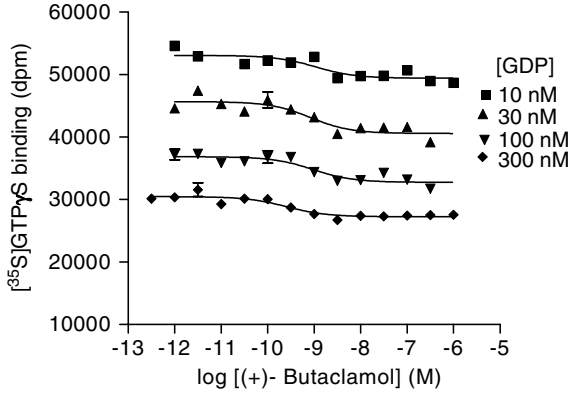

Figure 4 Effect of GDP on the inhibition of basal [^{35}S]GTPγS binding by (+)-butaclamol. Inhibition of [^{35}S]GTPγS binding by different concentrations of (+)-butaclamol was determined in the presence of different concentrations of GDP as described in Methods section. The data were fitted using a sigmoidal dose–response curve with a Hill coefficient of one. Curves are representative examples of data replicated as in Table 3.

Table 3 The effect of GDP concentration on inverse agonist potency

	pIC_{50} (IC_{50}, nM) efficacy (%)			
[GDP] nM	*10*	*30*	*100*	*300*
(+)-Butaclamol	8.83±0.08	9.02±0.09	9.05±0.06	9.37±0.16*
	(1.5)	(0.95)	(0.89)	(0.43)
	100	96	83	53
Spiperone	9.59±0.11	9.65±0.11	9.73±0.20	9.82±0.23
	(0.26)	(0.22)	(0.19)	(0.15)
	100	96	69	52
(−)-Sulpiride	6.98±0.21	6.75±0.15	6.80±0.09	7.03±0.24
	(105)	(178)	(158)	(93)
	100	91	62	38

Concentration/response experiments for inverse agonist inhibition of [^{35}S]GTPγS binding to membranes of CHO cells expressing D_2 receptors were performed in the presence of the indicated concentrations of GDP as described in Methods section. IC_{50} values were determined and are expressed as pIC_{50}±s.e.m. (three to five experiments). IC_{50} values are given in brackets. Data are also given for the mean efficacy for the compounds at each GDP concentration expressed as a percentage of the response (inhibition of [^{35}S]GTPγS binding) at 10 nM GDP.
*$P<0.05$ compared to 10 nM GDP.

Simulations of ligand-binding data using the extended ternary complex model

Simulations were carried out using the extended ternary complex model (Figure 1) in order to analyse the experimental data in more detail. The model was formulated for two competing ligands, an inverse agonist in competition with an agonist. Values for dissociation constants of the agonist were chosen to provide data similar to the saturation-binding data seen with [^{3}H]NPA. It was assumed that the agonist bound with higher affinity to the R* and R*G states than to the R state of the receptor, that is, $K_{R*G} = K_{R*} < K_R$. Values for these constants were as follows: $K_{R*G} = K_{R*} = 10^{-11}$ M, $K_R = 5 \times 10^{-9}$ M. It was also assumed that the affinity of the inverse agonist for R* and R*G receptor species was equivalent ($K_{R*} = K_{R*G}$) and that the ligand showed a higher affinity for R over these species ($K_R < K_{R*}$). Thus, the inverse agonist stabilises the receptor ground state over partially active R* and fully active R*G states. K_R for the inverse agonist was held constant at 1×10^{-10} M and K_{R*G} was varied to give the indicated K_{R*G}/K_R ratios (Figure 5).

Simulations were performed using these parameters for a single concentration of agonist (1 nM) and different competing concentrations of inverse agonist and the simulated data were analysed using Prism. In each case, the data fitted best to a two-binding site model from which values for $K_{uncoupled}$ and $K_{coupled}$ could be extracted (Table 4). From the simulated data, it is evident that the $K_{uncoupled}/K_{coupled}$ ratio derived from the analysis underestimates the K_{R*G}/K_R ratio. If the simulations are repeated, but with different values of J corresponding to different extents of R*/G coupling, then at high values of J, corresponding to weak receptor/G-protein coupling, $K_{uncoupled}/K_{coupled}$ tends to unity, whereas at low J values, corresponding to strong receptor/G-protein coupling, $K_{uncoupled}/K_{coupled}$ approaches the K_{R*G}/K_R ratio (Figure 6). These simulations show, therefore, that if there is some basal receptor/G-protein

Table 4 Simulated competition of a [^{3}H]agonist by an inverse agonist

K_R/K_{R*G}	5	10	20	40	80	160	320
$K_{uncoupled}$ (nM)	0.11	0.11	0.11	0.12	0.12	0.12	0.12
$K_{coupled}$ (nM)	0.28	0.41	0.54	0.65	0.73	0.77	0.80
$K_{uncoupled}/K_{coupled}$	2.55	3.73	4.91	5.41	6.08	6.42	6.67
$\%R_h$	36.3	36.8	37.2	37.6	37.8	37.9	38.0

The extended ternary complex model for two ligands was used with the following parameters: $R_{tot} = 1 \times 10^{-7}$ M, $G_{tot} = 5 \times 10^{-8}$ M, $L = 100$, $J = 1 \times 10^{-10}$ M; dissociation constants for inverse agonist: $K_R = 1 \times 10^{-10}$ M, $K_{R*} = K_{R*G}$; dissociation constants for agonist: $K_R = 5 \times 10^{-9}$ M, $K_{R*} = 1 \times 10^{-11}$ M, $K_{R*G} = 1 \times 10^{-11}$ M. K_{R*G} was varied to give the K_R/K_{R*G} ratios shown, data were simulated in Excel ([agonist] = 1 nM, varying concentrations of inverse agonist) and fitted using Prism as described in Methods section. Simulated data were fitted best by two-binding site models in all cases and values for $K_{uncoupled}$, $K_{coupled}$ and $\%R_h$ were derived as described in the text.

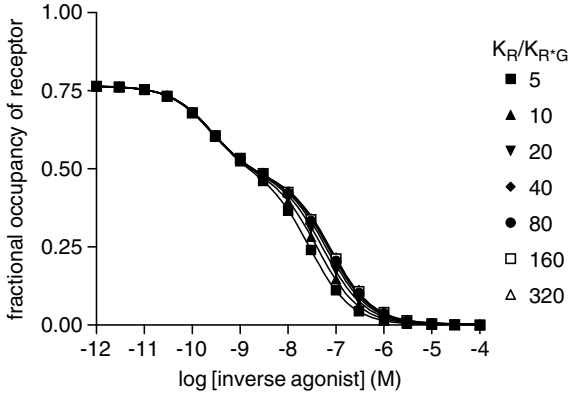

Figure 5 Simulation of inverse agonist/[^{3}H]agonist competition using the extended ternary complex model (Figure 1). The extended ternary complex model for two ligands was used with the following parameters: $R_{tot} = 1 \times 10^{-7}$ M, $G_{tot} = 5 \times 10^{-8}$ M, $L = 100$, $J = 1 \times 10^{-10}$ M; dissociation constants for inverse agonist: $K_R = 1 \times 10^{-10}$ M, $K_{R*} = K_{R*G}$; dissociation constants for agonist: $K_R = 5 \times 10^{-9}$ M, $K_{R*} = 1 \times 10^{-11}$ M, $K_{R*G} = 1 \times 10^{-11}$ M. K_{R*G} was varied to give the K_R/K_{R*G} ratios shown, data were simulated in Excel ([agonist] = 1 nM, varying concentrations of inverse agonist) and fitted using Prism as described in Methods section. Parameters derived from this analysis are given in Table 4.

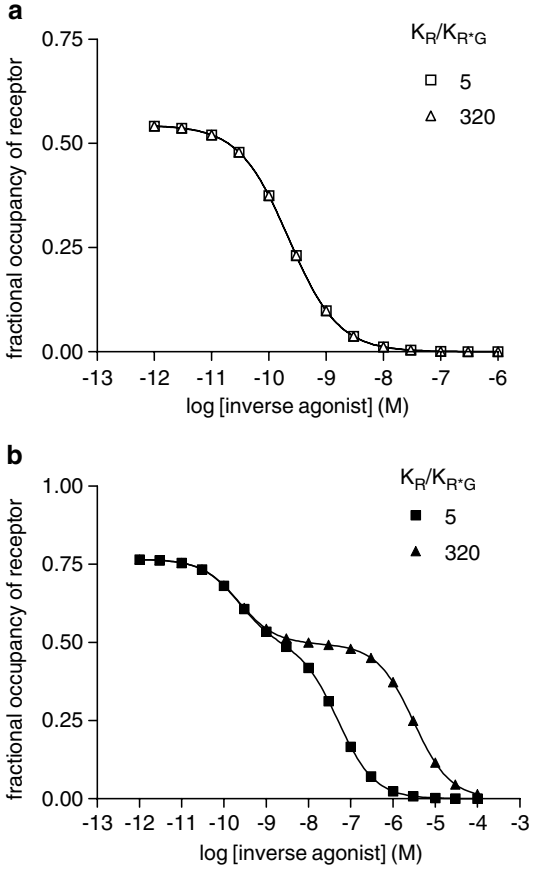

Figure 6 Simulation of inverse agonist/[^{3}H]agonist competition using the extended ternary complex model (Figure 1), effects of high and low J constant. The extended ternary complex model for two ligands was used with the following parameters: $R_{tot} = 1 \times 10^{-7}$ M, $G_{tot} = 5 \times 10^{-8}$ M, $L = 100$, $J = 1 \times 10^{-5}$ M (a) and 1×10^{-13} M (b); dissociation constants for inverse agonist: $K_R = 1 \times 10^{-10}$ M, $K_{R*} = K_{R*G}$; dissociation constants for agonist: $K_R = 5 \times 10^{-9}$ M, $K_{R*} = 1 \times 10^{-11}$ M, $K_{R*G} = 1 \times 10^{-11}$ M. K_{R*G} was varied to give the K_R/K_{R*G} ratios shown, data were simulated in Excel ([agonist] = 1 nM, varying concentrations of inverse agonist) and fitted using Prism as described in Methods section.

coupling, it is possible to detect discrimination between G-protein-coupled and -uncoupled forms of the receptor in these assays. Values of $K_{coupled}$ will, however, be underestimated unless receptor/G-protein coupling is strong. The simulations also show clearly that if the extended ternary complex model holds, competition between an inverse agonist and an agonist (parameters chosen to model the present experimental data set) should follow a two-binding site model with $\%R_H$ approximately 40%.

Simulations as in Figures 5 and 6 were also performed where, for the inverse agonist $K_{R^*G} > K_{R^*} = K_R$, with very similar results.

Discussion

In this study, we have probed the mechanism of inverse agonism at D_2 dopamine receptors in a series of ligand-binding and functional experiments combined with simulations of data. The results provide evidence that some inverse agonists function by stabilising the receptor uncoupled from G proteins, whereas for others the mechanism could not be defined. Understanding the mechanisms of inverse agonism at D_2 dopamine receptors is important as many of the inverse agonists tested are used therapeutically for the treatment of schizophrenia.

As outlined in the Introduction, there are several possible mechanisms for inverse agonism at GPCRs. In previous work we examined the mechanisms of inverse agonism at the D_2 dopamine receptor in two ways. A mutant D_2 dopamine receptor (T343R) was examined and shown to possess the properties of a receptor that lies towards the activated conformation (Wilson *et al*., 2001). Agonist affinities were increased for this receptor relative to the native receptor, but the affinities of inverse agonists were unchanged. In a second study (Roberts *et al*., 2004), the dissociation constants of a range of inverse agonists were determined in competition experiments *versus* the inverse agonist [^{3}H]spiperone and *versus* the agonist [^{3}H]NPA. Affinities of inverse agonists were similar when determined *versus* the two radioligands. From these observations, it might be concluded that inverse agonists at the D_2 receptor do not discriminate the different states of the receptor (R, R*, R*G). These experimental approaches have limitations. For example, the affinities of inverse agonists will be affected by mutations only if the mutation strongly favours the activated state (Wade *et al*., 2001). Also, in using two radioligands to assess inverse agonist affinities at coupled and uncoupled states, any differences in behaviour of the two radioligands may obscure small differences in affinity for the inverse agonist between the two states. Therefore, in the present study, we used the agonist radioligand [^{3}H]NPA to examine the affinities of inverse agonists for the different states of the receptor. [^{3}H]NPA is a radioligand that will bind to both the coupled and uncoupled forms of the receptor with different, but high affinity, so that labelling of both sets of sites may be examined in a single ligand-binding assay.

Indeed, in the present study, when a sufficiently high concentration of the radioligand was used, inverse agonist/[^{3}H]NPA competition experiments gave data that were fitted best by a two-binding site model. It is assumed that the two sites represent competition *versus* [^{3}H]NPA from its lower-affinity (G-protein-uncoupled) and higher-affinity (G-protein-coupled) binding sites. This assumption was confirmed in experiments performed in the presence of GTP to uncouple receptor and G protein when the data were fitted best by a one-binding site model. When dissociation constants for the two sites were determined, a significant difference between the sets of $K_{coupled}$ and $K_{uncoupled}$ values was seen, but these parameters were significantly different in a *post hoc* test only for (+)-butaclamol. When this comparison was made, but omitting the data for (+)-butaclamol, the sets of $K_{coupled}$ and $K_{uncoupled}$ values were still significantly different, but no values were different in a *post hoc* test. K_{iGTP} values derived from experiments in the presence of GTP were not significantly different from values for $K_{uncoupled}$, but were significantly different from values for $K_{coupled}$ (although see below). These data show clearly that (+)-butaclamol does discriminate between R/R* and R*G receptor states. It cannot, however, be concluded that other inverse agonists do not show such a discrimination as there is a significant difference (ANOVA) between the $K_{coupled}$ and $K_{uncoupled}$ data sets.

The percentage of higher-affinity sites ($\%R_H$) in these analyses was found to vary somewhat. For many of the compounds tested this figure was ~40%, but for spiperone and (+)-butaclamol the figure was ~75%. In some cases, better fits to the data were obtained with values of the $\%R_H$ constrained, but no clear pattern emerged. Nevertheless, it seems that there is variability in this parameter and this would not be expected for a ternary complex model. Indeed, we have performed simulations of such data with the extended model, but do not see such large changes in $\%R_H$. It seems, therefore, that there is additional complexity in the interaction of inverse agonists with this receptor not contained in these models.

The relative efficacy of the different compounds as inverse agonists was determined from their ability to reduce basal [^{35}S]GTPγS binding. To obtain an inverse agonist signal in this assay, it was necessary to omit sodium ions from the buffer. It is believed that sodium ions help stabilise GPCRs in the ground state (Costa *et al*., 1992; Tian *et al*., 1994; Selley *et al*., 2000). The omission of sodium ions should, therefore, increase constitutive receptor/G-protein coupling and hence agonist-independent [^{35}S]GTPγS binding. Inverse agonist signals were also greater when assays were performed with either no GDP or low concentrations thereof. GDP is normally present in [^{35}S]GTPγS-binding assays in order to reduce basal receptor/G-protein coupling by occupying guanine nucleotide-free G-proteins, thus suppressing receptor/G-protein interaction. Removing GDP causes an increase in receptor/G-protein association and agonist-independent activation (Pauwels *et al*., 1997; Breivogel *et al*., 1998; McLoughlin & Strange, 2000) and the extent of inverse agonism may be modulated by changing the GDP concentration in assays (McLoughlin & Strange, 2000). Using these conditions, it was possible to observe inverse agonist effects with all of the compounds tested. Whereas for most of the compounds tested the extent of inverse agonism was similar to that seen with (+)-butaclamol, for quetiapine, raclopride and sulpiride, significantly lower relative efficacies were observed ($P<0.05$).

The relative efficacies of the inverse agonists tested here have been assessed using stimulation of adenylyl cyclase (Hall & Strange, 1997; Kozell & Neve, 1997; Wilson *et al*., 2001), [^{35}S]GTPγS binding (Wiens *et al*., 1998; Gilliland & Alper, 2000; Gazi *et al*., 2003) and phospholipase C activation in a chimeric D_2 dopamine/α_1 adrenergic receptor (Wurch *et al*.,

2003). In general, full inverse agonism has been observed for all the compounds tested here, although partial inverse agonist effects have been reported in one study (Kozell & Neve, 1997) and neutral antagonism has been reported for ziprasidone (Gazi *et al*., 2003; Wurch *et al*., 2003). The origin of these differences is unclear, but it could reflect differences in the systems used for the different measurements.

The fact that inverse agonism can be observed in the absence of GDP shows that the mechanism of inverse agonism does not simply involve the inhibition of GDP release. Therefore, a receptor-bound inverse agonist produces a receptor conformation that reduces the rate of [^{35}S]GTPγS binding to guanine nucleotide-free G-proteins. It can be inferred that the receptor conformation favoured by the inverse agonist either discourages receptor/G-protein coupling or allows for G-protein coupling, but prevents the G-protein from binding [^{35}S]GTPγS efficiently.

In order to probe the mechanisms of these inverse agonist effects further, we performed inverse agonist concentration/response experiments at different concentrations of GDP. For the 5-HT$_{1A}$ serotonin receptor, we have shown that this assay design discriminates among agonists and inverse agonists according to whether they do, or do not, bind differentially to different states of the receptor (G-protein-coupled or uncoupled) (McLoughlin & Strange, 2000). If the compound tested does bind differentially to these different states of the receptor, then its EC$_{50}$/IC$_{50}$ is affected by the changes in GDP. When such assays were performed for the D$_2$ dopamine receptor and the inverse agonists tested here, no significant change in IC$_{50}$ was observed for the inverse agonists spiperone or (−)-sulpiride. However, a significant change in potency was found for (+)-butaclamol. The change in potency was in good agreement with the $K_{uncoupled}$ and $K_{coupled}$ values calculated in competition against [^{3}H]-NPA. When the effects of GDP on inverse agonist potency were analysed by linear regression, a significant effect of GDP was seen for both (+)-butaclamol and for spiperone.

It appears, therefore, that (+)-butaclamol is able to redistribute the different states in the extended ternary complex model. It displays both decreased affinity for G-protein-coupled receptors as compared to G-protein-uncoupled receptors and an increase in potency when ternary complex formation is made less favourable (increased GDP). There is also some evidence based on the effects of GDP on inverse agonist potency that spiperone may redistribute these states. Little conclusive evidence emerged from the present study to suggest that the other ligands tested display this behaviour. Simulations of data (Figure 5) showed that, for compounds that bind differentially to R and R* states, unless there was very strong stabilisation of receptor/G-protein coupling, the determinations of $K_{coupled}$ and $K_{uncoupled}$ underestimated the discrimination. Nevertheless, for two compounds examined in the present study, we have been able to demonstrate discrimination between different states of the receptor. This shows that there must be some constitutive receptor/G-protein coupling and that for two compounds the mechanism of inverse agonism derives from discrimination of ground and activated states of the receptor. For the other compounds tested, we are unable to discriminate the different mechanisms of inverse agonism outlined in the Introduction.

For other receptors, for example, α_{1A} and α_{1B} adrenergic receptors, 5-HT$_{1A}$ serotonin receptor (Rossier *et al*., 1999; McLoughlin & Strange, 2000), it has been shown that inverse agonism may occur in the absence of redistribution of receptor states. Indeed, a recent study has characterised a 5-HT$_{2C}$ receptor mutant that would appear to be fixed in the active conformation (Prioleau *et al*., 2002). While large increases in agonist affinity were observed for this mutant receptor as compared to the native (40–100-fold), only a few of the inverse agonists tested showed any change in affinity (<5-fold reduction) and most inverse agonists tested showed no detectable change. This is further evidence to suggest that not all inverse agonists act by redistributing R, R* and R*G states.

In conclusion, a number of antagonists at the D$_2$ receptor have been classified as inverse agonists in a [^{35}S]GTPγS-binding assay in the absence of sodium ions or GDP. Evidence has been presented which shows that (+)-butaclamol and spiperone may bind preferentially to receptors uncoupled from G protein. For the other compounds tested, there is a significant difference between the sets of affinities for these compounds for the coupled and uncoupled states. Hence, although there is no direct evidence that these compounds do bind preferentially to uncoupled receptors, this cannot be discounted based on the present study.

We thank the Wellcome Trust for financial support, Claire Carter for giving us the Excel version of the Extended Ternary Complex model and Dr Martyn Wood (G.S.K.) for the generous gift of ziprasidone.

References

AKAM, E. & STRANGE, P.G. (2004). Inverse agonist properties of atypical antipsychotic drugs. *Biochem. Pharmacol.,* **67,** 2039–2045.

ALDER, J.T., HACKSELL, U. & STRANGE, P.G. (2003). Analysis of molecular determinants of affinity and relative efficacy of a series of *R*- and *S*-2-(dipropylamino)tetralins at the 5-HT1A serotonin receptor. *Br. J. Pharmacol.,* **138,** 1129–1139.

ALEWIJNSE, A.E., SMIT, M.J., HOFFMANN, M., VERZIJL, D., TIMMERMAN, H. & LEURS, R. (1998). Constitutive activity and structural instability of the wild-type human H2 receptor. *J. Neurochem.,* **71,** 799–807.

BOUABOULA, M., DESNOYER, N., CARAYON, P., COMBES, T. & CASELLAS, P. (1999). Gi protein modulation induced by a selective inverse agonist for the peripheral cannabinoid receptor CB2: implication for intracellular signalization cross-regulation. *Mol. Pharmacol.,* **55,** 473–480.

BOUABOULA, M., PERRACHON, S., MILLIGAN, L., CANAT, X., RINALDI-CARMONA, M., PORTIER, M., BARTH, F., CALANDRA, B., PECCEU, F., LUPKER, J., MAFFRAND, J.P., LE FUR, G. & CASELLAS, P. (1997). A selective inverse agonist for central cannabinoid receptor inhibits mitogen-activated protein kinase activation stimulated by insulin or insulin-like growth factor 1. Evidence for a new model of receptor/ligand interactions. *J. Biol. Chem.,* **272,** 22330–22339.

BREIVOGEL, C.S., SELLEY, D.E. & CHILDERS, S.R. (1998). Cannabinoid receptor agonist efficacy for stimulating [^{35}S]GTPgammaS binding to rat cerebellar membranes correlates with agonist-induced decreases in GDP affinity. *J. Biol. Chem.,* **273,** 16865–16873.

CASTRO, S.W. & STRANGE, P.G. (1993). Differences in the ligand binding properties of the short and long versions of the D2 dopamine receptor. *J. Neurochem.,* **60,** 372–375.

CHENG, Y. & PRUSOFF, W.H. (1973). Relationship between the inhibition constant (K1) and the concentration of inhibitor which causes 50 per cent inhibition (I50) of an enzymatic reaction. *Biochem. Pharmacol.,* **22,** 3099–3108.

COSTA, T. & HERZ, A. (1989). Antagonists with negative intrinsic activity at delta opioid receptors coupled to GTP-binding proteins. *Proc. Natl. Acad. Sci. U.S.A.,* **86,** 7321–7325.

COSTA, T., OGINO, Y., MUNSON, P.J., ONARAN, H.O. & RODBARD, D. (1992). Drug efficacy at guanine nucleotide-binding regulatory protein-linked receptors: thermodynamic interpretation of negative antagonism and of receptor activity in the absence of ligand. *Mol. Pharmacol.,* **41,** 549–560.

GARDNER, B.R., HALL, D.A. & STRANGE, P.G. (1997). Agonist action at D2(short) dopamine receptors determined in ligand binding and functional assays. *J. Neurochem.,* **69,** 2589–2598.

GAZI, L., NICKOLLS, S.A. & STRANGE, P.G. (2003). Functional coupling of the human dopamine D2 receptor with G alpha i1, G alpha i2, G alpha i3 and G alpha o G proteins: evidence for agonist regulation of G protein selectivity. *Br. J. Pharmacol.,* **138,** 775–786.

GETHER, U. & KOBILKA, B.K. (1998). G protein-coupled receptors. II. Mechanism of agonist activation. *J. Biol. Chem.,* **273,** 17979–17982.

GILLILAND, S.L. & ALPER, R.H. (2000). Characterization of dopaminergic compounds at hD2short, hD4.2 and hD4.7 receptors in agonist-stimulated [^{35}S]GTPgammaS binding assays. *Naunyn-Schmiedeberg's Arch. Pharmacol.,* **361,** 498–504.

HALL, D.A. & STRANGE, P.G. (1997). Evidence that antipsychotic drugs are inverse agonists at D2 dopamine receptors. *Br. J. Pharmacol.,* **121,** 731–736.

KOZELL, L.B. & NEVE, K.A. (1997). Constitutive activity of a chimeric D2/D1 dopamine receptor. *Mol. Pharmacol.,* **52,** 1137–1149.

LEFF, P., SCARAMELLINI, C., LAW, C. & MCKECHNIE, K. (1997). A three-state receptor model of agonist action. *Trends Pharmacol. Sci.,* **18,** 355–362.

LEFKOWITZ, R.J., COTECCHIA, S., SAMAMA, P. & COSTA, T. (1993). Constitutive activity of receptors coupled to guanine nucleotide regulatory proteins. *Trends Pharmacol. Sci.,* **14,** 303–307.

LOWRY, O., ROSEBROUGH, N., FARR, A. & RANDALL, R. (1951). Protein measurement with the folin phenol reagent. *J. Biol. Chem.,* **193,** 265–275.

MCLOUGHLIN, D.J. & STRANGE, P.G. (2000). Mechanisms of agonism and inverse agonism at serotonin 5-HT1A receptors. *J. Neurochem.,* **74,** 347–357.

PAUWELS, P.J., TARDIF, S., WURCH, T. & COLPAERT, F.C. (1997). Stimulated [^{35}S]GTP gamma S binding by 5-HT1A receptor agonists in recombinant cell lines. Modulation of apparent efficacy by G-protein activation state. *Naunyn-Schmiedeberg's Arch. Pharmacol.,* **356,** 551–561.

PRIOLEAU, C., VISIERS, I., EBERSOLE, B.J., WEINSTEIN, H. & SEALFON, S.C. (2002). Conserved helix 7 tyrosine acts as a multistate conformational switch in the 5HT2C receptor. Identification of a novel 'locked-on' phenotype and double revertant mutations. *J. Biol. Chem.,* **277,** 36577–36584.

ROBERTS, D., LIN, H. & STRANGE, P. (2004). Investigation of the mechanism of agonist and inverse agonist action at D_2 dopamine receptors. *Biochem. Pharmacol.,* **67,** 1657–1665.

ROSSIER, O., ABUIN, L., FANELLI, F., LEONARDI, A. & COTECCHIA, S. (1999). Inverse agonism and neutral antagonism at alpha(1a)- and alpha(1b)-adrenergic receptor subtypes. *Mol. Pharmacol.,* **56,** 858–866.

SAMAMA, P., COTECCHIA, S., COSTA, T. & LEFKOWITZ, R.J. (1993). A mutation-induced activated state of the beta 2-adrenergic receptor. Extending the ternary complex model. *J. Biol. Chem.,* **268,** 4625–4636.

SELLEY, D.E., CAO, C.C., LIU, Q. & CHILDERS, S.R. (2000). Effects of sodium on agonist efficacy for G-protein activation in mu-opioid receptor-transfected CHO cells and rat thalamus. *Br. J. Pharmacol.,* **130,** 987–996.

SIBLEY, D.R., DE LEAN, A. & CREESE, I. (1982). Anterior pituitary dopamine receptors. Demonstration of interconvertible high and low affinity states of the D-2 dopamine receptor. *J. Biol. Chem.,* **257,** 6351–6361.

STRANGE, P.G. (2001). Antipsychotic drugs: importance of dopamine receptors for mechanisms of therapeutic actions and side effects. *Pharmacol. Rev.,* **53,** 119–133.

STRANGE, P.G. (2002). Mechanisms of inverse agonism at G-protein-coupled receptors. *Trends Pharmacol. Sci.,* **23,** 89–95.

TIAN, W.N., DUZIC, E., LANIER, S.M. & DETH, R.C. (1994). Determinants of alpha 2-adrenergic receptor activation of G proteins: evidence for a precoupled receptor/G protein state. *Mol. Pharmacol.,* **45,** 524–531.

WADE, S.M., LAN, K., MOORE, D.J. & NEUBIG, R.R. (2001). Inverse agonist activity at the alpha(2A)-adrenergic receptor. *Mol. Pharmacol.,* **59,** 532–542.

WIENS, B.L., NELSON, C.S. & NEVE, K.A. (1998). Contribution of serine residues to constitutive and agonist-induced signaling *via* the D2S dopamine receptor: evidence for multiple, agonist-specific active conformations. *Mol. Pharmacol.,* **54,** 435–444.

WILSON, J., LIN, H., FU, D., JAVITCH, J.A. & STRANGE, P.G. (2001). Mechanisms of inverse agonism of antipsychotic drugs at the D(2) dopamine receptor: use of a mutant D(2) dopamine receptor that adopts the activated conformation. *J. Neurochem.,* **77,** 493–504.

WURCH, T., BOUTET-ROBINET, E.A., PALMIER, C., COLPAERT, F.C. & PAUWELS, P.J. (2003). Constitutive coupling of a chimeric dopamine D2/alpha 1B receptor to the phospholipase C pathway: inverse agonism to silent antagonism by neuroleptic drugs. *J. Pharmacol. Exp. Ther.,* **304,** 380–390.

(Received June 3, 2004
Revised October 22, 2004
Accepted October 26, 2004)